Національна академія наук України

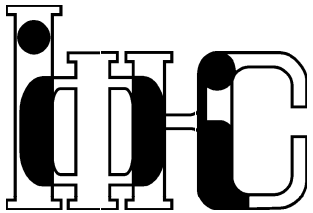

ІНСТИТУТ ФІЗИКИ КОНДЕНСОВАНИХ СИСТЕМ

ICMP–05–10E

M.Druchok, Yu.Kalyuzhnyi, J.Reščič* and V.Vlachy*

Analysis of osmotic pressure data for aqueous protein solutions via a multi-component model

*Faculty of Chemistry and Chemical Technology, University of Ljubljana,1000 Ljubljana, Slovenia

ЛЬВІВ

УДК: 532, 532.772, 532.74

PACS: 61.20.Gy, 61.20.Ja, 61.20.Qg

Аналіз даних для осмотичного тиску водних розчинів протеїнів на основі багатокомпонентної моделі

М. Дручок, Ю. Калюжний, Ю. Рещіч, В. Влахі

Анотація. Проведено дослідження рівноваги Донана. Електроліт змодельовано протеїнами у формах мономерів і димерів, ко- і контріонами, що представлені зарядженими твердими сферами різного розміру і заряду. Для вивчення властивостей моделі було використано розв'язок рівняння Орнштейна-Церніке у асоціативних середньосферичному і гіперланцюжковому наближеннях. Для перевірки теорії проведено моделювання методом Монте-Карло моделі водного розчину протеїну лізоциму при 0.1-мольному буфері NaCl. Запропоновану теорію було застосовано до опису низки експериментальних даних осмотичного тиску для протеїнів *bovine serum albumin* в 0.15-мольному буфері NaCl, *human serum albumin* в 0.1-мольному фосфатному буфері і лізоциму в сульфатному і фосфатному буферах.

Analysis of osmotic pressure data for aqueous protein solutions via a multi-component model

M.Druchok, Yu.Kalyuzhnyi, J.Reščič and V.Vlachy

Abstract. A Donnan equilibrium for a series of systems is studied. In order to describe the unusually low osmotic pressure in many experiments we assumed protein molecules can form dimers. The model solution contains proteins in monomeric or dimerized forms, co- and counterions, which are modelled as charges spheres. The associative mean spherical and hypernetted chain approximations were applied to this model. In order to test the theory a Monte Carlo simulations were performed for the model mimicking lysozyme solution in 0.1M sodium chloride buffer. Using the theoretical approaches mentioned above we analyzed experimental data for the osmotic pressure of bovine serum albumin in 0.15M sodium chloride, human serum albumin solution in 0.1M phosphate buffer and lysozyme in sulphate and phosphate buffers.

1. Introduction

A variety of phenomena which are of interest for basic sciences and technology occur in systems consisting of two ionic solutions separated by a semipermeable membrane. The actual applications range from waste water treatment (see, for example, [1]) to drug delivery [2]. In addition membrane osmometry is often used to identify the principal interactions in protein solutions (see, [3–9]).

Proteins are often pictured as highly asymmetric electrolytes; their properties are influenced by attractive interaction between a protein molecule and oppositely charged small ions (counterions) in the solution. This attraction leads to accumulation of counterions in the vicinity of proteins. Due to electrostatic repulsion the small ions carrying the charge of the same sign as proteins (called co-ions)are pushed away from the protein. This effect is an origin of the so–called Donnan electrolyte exclusion [10]. Presence of high concentration of simple electrolyte affects stability of these systems; in addition to concentration the composition of added electrolyte is also important. It is the valency of counterions which matters - the solutions containing divalent or trivalent counterions are less stable than those having monovalent counterions. Further, chemical nature of the ions present in a system may play a role in shaping the properties of protein solutions. For this reason the potential of mean force between proteins is difficult to model [11] (see also [12–14]). There are other features which separate proteins from somehow simpler colloidal or micellar systems, for example, protein molecules posses an ability to form dimers. The main purpose of present study is to explore the effect of presence of dimerized protein to thermodynamic and structural properties of these solutions.

A model solution in which protein molecules can exist in forms of monomers and dimers has been preliminary investigated for the simple electrolyte–free systems using the integral equation technique. The results published in reference [15] indicate that the short–range attraction between proteins, and consequently a formation of dimers, yields a significant decrease of the osmotic pressure for the model protein solution. In the paper mentioned above, solutions containing only proteins and counterions were investigated. A more interesting and also more realistic case (proteins are not stable in water) would consider protein – electrolyte (buffer) mixture.

In the present contribution we consider the equilibrium between simple electrolyte on one and electrolyte–protein mixture on the other side of the semi–permeable membrane. The difference in osmotic pressures

across the membrane can be measured experimentally [3, 8, 9]; this is so–called Donnan pressure. In what follows we present new computer simulations and integral equation calculations for model protein – electrolyte mixtures where 'protein' molecules can form dimers. Both thermodynamic (excess internal energy, Donnan pressure) and structural parameters (distribution functions) are calculated for various fractions of protein dimers in the system. The validity of integral–equation theories is assessed by comparison with the new Monte Carlo simulations for the same model while, on the other hand, these theories are used to analyze experimental data for Donnan pressure in several protein systems.

2. Modelling of Protein in Solution

In the present calculation the ions are pictured as hard spheres carrying different charges and of various sizes. We consider a multi–component solution containing (i) multivalent spherical protein molecules p with the charge eZ_p, diameter σ_p and number density ρ_p, (ii) small spherical counterions c with the charge eZ_c, diameter σ_c and number density ρ_c and (iii) small co-ions a with the charge eZ_a, diameter σ_a and number density ρ_a. Here e denotes the elementary charge and the solvent is represented as a continuum with dielectric constant $\epsilon = 78.5$. The charges are assumed to be located in centers of spherical particles. The pair potential acting between the centers α and β (we only consider those belonging to different particles) is

$$U_{\alpha\beta}(r) = U^{HS}_{\alpha\beta}(r) + U^{C}_{\alpha\beta}(r) \tag{2.1}$$

where

$$\begin{aligned} U^{HS}_{\alpha\beta}(r) &= \begin{cases} \infty, & r \le \sigma_{\alpha\beta} = (\sigma_\alpha + \sigma_\beta)/2 \\ 0, & r > \sigma_{\alpha\beta} = (\sigma_\alpha + \sigma_\beta)/2 \end{cases}, \\ U^{C}_{\alpha\beta}(r) &= Z_\alpha Z_\beta e^2/(4\pi\epsilon_0\epsilon r). \end{aligned}$$

To account a protein association we assume, that certain number of protein molecules (their number density is ρ_d) form dimers. In other words, the fraction of protein molecules $x_p = \rho_d/\rho_p$ is dimerized, i.e. they form a rigid dimer with the distance between centers $L = \sigma_p$. The number density of dimers is therefore equal to $\rho_d/2$, and if we denote the number density of monomers by ρ_m we obtain the equality $\rho_p = \rho_m + \rho_d$.

The electroneutrality condition

$$\sum_\alpha \rho_\alpha Z_\alpha = 0 \tag{2.2}$$

applies for the system, where subscript α can be p, c and a, denoting the species in solution.

3. Integral Equation Theory

The model of protein solution described above was solved to obtain structural and thermodynamic properties using two-density theory for site-site interaction [16–18]. The corresponding Ornstein–Zernike (OZ) equation for this system reads:

$$\mathbf{H}_{\alpha\beta}(\mathbf{r_{12}}) = \mathbf{C}_{\alpha\beta}(\mathbf{r_{12}}) + \sum_{\eta} \int \mathbf{C}_{\alpha\eta}(\mathbf{r_{13}}) \boldsymbol{\rho}_{\eta} \mathbf{H}_{\eta\beta}(\mathbf{r_{32}}) \mathbf{dr_3} \qquad (3.1)$$

where $\mathbf{H}_{\alpha\beta}$, $\mathbf{C}_{\alpha\beta}$, and $\boldsymbol{\rho}_{\eta}$ are the matrices of the following form

$$\mathbf{H}_{\alpha\beta} = \begin{bmatrix} h^{00}_{\alpha\beta} & h^{01}_{\alpha\beta} \\ h^{10}_{\alpha\beta} & h^{11}_{\alpha\beta} \end{bmatrix}, \mathbf{C}_{\alpha\beta} = \begin{bmatrix} c^{00}_{\alpha\beta} & c^{01}_{\alpha\beta} \\ c^{10}_{\alpha\beta} & c^{11}_{\alpha\beta} \end{bmatrix}, \boldsymbol{\rho}_{\alpha} = \begin{bmatrix} \rho_{\alpha} & \rho_{\alpha} \\ \rho_{\alpha} & 0 \end{bmatrix},$$

Here $c^{\alpha\beta}_{ij}(r)$ and $h^{\alpha\beta}_{ij}(r)$ are direct and total correlation functions, respectively. Subscripts α and β denote species and stand for $\alpha, \beta = m, c, a, d$ and upper indices denote bonding states. In this way $i = 0$ correspond to non–bonded state and $i = 1$ to the bonded state [17,18]. Relation between the site–site radial distribution function $g_{\alpha\beta}(r)$ and partial radial distribution functions is

$g^{ij}_{\alpha\beta}(r) = h^{ij}_{\alpha\beta}(r) + \delta_{i0}\delta_{j0}$ and

$$g_{\alpha\beta}(r) = \sum_{ij} g^{ij}_{\alpha\beta} \qquad (3.2)$$

where δ_{ij} is the Kroneker delta.

The set of Ornstein–Zernike equations (3.1) has to be supplemented by the additional relation between direct and total correlation functions. In this study we are using polymer hypernetted–chain (PHNC) approximation and polymer mean spherical approximation (PMSA), which are briefly described in the next Section.

3.1. Polymer HNC Closure

Polymer hypernetted–chain closure equations can be written in the following form [17,18]

$$g^{00}_{\alpha\beta}(r) = \exp(-\beta U_{\alpha\beta}(r) + t^{00}_{\alpha\beta}(r)),$$

$$\begin{aligned} g^{01}_{\alpha\beta}(r) &= g^{00}_{\alpha\beta}(r) t^{01}_{\alpha\beta}(r), \\ g^{10}_{\alpha\beta}(r) &= g^{00}_{\alpha\beta}(r) t^{10}_{\alpha\beta}(r), \\ g^{11}_{\alpha\beta}(r) &= g^{00}_{\alpha\beta}(r)[t^{01}_{\alpha\beta}(r) t^{10}_{\alpha\beta}(r) + t^{11}_{\alpha\beta}(r)] + \Delta^{11}_{\alpha\beta}(r), \end{aligned} \qquad (3.3)$$

where

$$\Delta^{ij}_{\alpha\beta}(r) = \delta_{i1}\delta_{j1} \frac{\delta_{\alpha p}\delta_{\beta p}}{4\pi\rho_d\sigma^2_{pp}} \delta(r - \sigma_{pp}), \qquad (3.4)$$

$\delta(x)$ is the Dirac delta-function and $t^{ij}_{\alpha\beta}(r) = h^{ij}_{\alpha\beta}(r) - c^{ij}_{\alpha\beta}(r)$.

The Ornstein–Zernike equations (3.1) together with PHNC closure relations (3.3) form a closed set of equations to be solved numerically. Once the solution is obtained it can be used to calculate thermodynamic properties for the model solution, including the excess Helmholtz free energy F^{ex}, excess chemical potential μ^{ex}_{α}, and excess osmotic pressure P^{ex}. The relevant expressions are [17–19]

$$\begin{aligned} -\beta\frac{F^{ex}}{V} = \frac{1}{2}\sum_{\alpha\beta}\int d\mathbf{r}\, \left\{ \left[\boldsymbol{\rho}_{\alpha}\tilde{\mathbf{C}}_{\alpha\beta}(r)\boldsymbol{\rho}_{\beta}\right]^{00} - \frac{1}{2}\mathrm{Tr}\left[\boldsymbol{\rho}_{\alpha}\tilde{\mathbf{H}}_{\alpha\beta}(r)\boldsymbol{\rho}_{\beta}\tilde{\mathbf{H}}_{\beta\alpha}(r)\right]\right\} \\ -\frac{1}{16\pi^3}\int d\mathbf{k}\, \sum_{\alpha}\mathrm{Tr}\left[\boldsymbol{\rho}_{\alpha}\tilde{\mathbf{C}}_{\alpha\alpha}(k) + \sum_{\beta}\boldsymbol{\rho}_{\alpha}\boldsymbol{\Delta}_{\alpha\beta}(k)\boldsymbol{\rho}_{\beta}\tilde{\mathbf{C}}_{\beta\alpha}(k)\right] \\ -\frac{1}{16\pi^3}\int d\mathbf{k}\ln\det\left[\mathbf{1} - \boldsymbol{\rho}\mathbf{C}(\mathbf{k})\right] \end{aligned} \qquad (3.5)$$

$$-\beta\rho_{\alpha}\mu^{ex}_{\alpha} = \sum_{\beta}\int d\mathbf{r}\, \left\{ \left[\boldsymbol{\rho}_{\alpha}\tilde{\mathbf{C}}_{\alpha\beta}(r)\boldsymbol{\rho}_{\beta}\right]^{00} - \frac{1}{2}\mathrm{Tr}\left[\boldsymbol{\rho}_{\alpha}\tilde{\mathbf{H}}_{\alpha\beta}(r)\boldsymbol{\rho}_{\beta}\mathbf{T}_{\beta\alpha}(r)\right]\right\}, \qquad (3.6)$$

$$\beta P^{ex} = -\beta\frac{F^{ex}}{V} + \sum_{\alpha}\beta\rho_{\alpha}\mu^{ex}_{\alpha}, \qquad (3.7)$$

where the following notation is used: $\tilde{\mathbf{C}}_{\alpha\beta}(r) = \mathbf{C}_{\alpha\beta}(\mathbf{r}) - \boldsymbol{\Delta}_{\alpha\beta}(\mathbf{r})$, $\mathbf{C}(k)$ and $\boldsymbol{\rho}$ are the matrices with the elements $\mathbf{C}_{\alpha\beta}(k)$ and $\boldsymbol{\rho}_{\alpha}$, respectively while $[...]^{00}$ denotes 00 element of the corresponding matrix.

3.2. Polymer MSA Closure

Polymer mean spherical approximation is a multi–density version of the regular mean spherical theory. For the model studied here we have [20,21]

$$\begin{cases} c^{ij}_{\alpha\beta}(r) = -\beta\delta_{i0}\delta_{j0}U^{C}_{\alpha\beta}(r) + \Delta^{ij}_{\alpha\beta}(r), & r \geq \sigma_{\alpha\beta} = (\sigma_{\alpha} + \sigma_{\beta})/2 \\ h^{ij}_{\alpha\beta}(r) = -\delta_{i0}\delta_{j0}, & r < \sigma_{\alpha\beta} = (\sigma_{\alpha} + \sigma_{\beta})/2 \end{cases}, \qquad (3.8)$$

Solution of the Ornstein–Zernike equation with the polymer mean spherical closure has been derived earlier for the general case of the multicomponent mixture of charged chain-like molecules [21]. For this reason we omit the details of derivation here, and only present the final expressions relevant for our model. The solution of polymer MSA [21] can be reduced to the solution of one single nonlinear algebraic equation for the scaling parameter Γ as introduced by Blum [22,23]. For our model the equation for Γ takes the following form

$$\Gamma^2 = \pi\beta^* \sum_\alpha \rho_\alpha \left[\Gamma_\alpha \left(z_\alpha - \frac{\pi\sigma_\alpha^2 \tilde{P}_n}{2\Delta + \pi\tilde{\Omega}_n} \right) \right]^2 + \pi\beta^* \rho_d \Gamma_d^3 \left(z_p - \frac{\pi\sigma_p^2 \tilde{P}_n}{2\Delta + \pi\tilde{\Omega}_n} \right)^2 \tag{3.9}$$

where $\beta^* = e\beta/\epsilon$, $\Delta = 1 - \pi/6 \sum_\alpha \rho_\alpha \sigma_\alpha^3$, $\Gamma_\alpha = (1 + \sigma_\alpha \Gamma)^{-1}$,

$$\tilde{P}_n = \sum_\alpha \rho_\alpha \sigma_\alpha z_\alpha \Gamma_\alpha + \frac{1}{2}\rho_d \sigma_p z_p \Gamma_p^2, \qquad \tilde{\Omega}_n = \sum_\alpha \rho_\alpha \sigma_\alpha^3 \Gamma_\alpha + \frac{1}{2}\rho_d \sigma_p^3 \Gamma_p^2 \tag{3.10}$$

Knowledge of the scaling parameter Γ allows one to calculate thermodynamic properties of the model. Following Bernard and Blum [24, 25], we have

$$\beta \frac{U^{el}}{V} = -\beta^* \left[\Gamma \sum_\alpha \rho_\alpha z_\alpha^2 \Gamma_\alpha - \frac{1}{2}\rho_d \frac{z_p^2 \Gamma_p^2}{\sigma_p} + \frac{\pi \tilde{P}_n^2}{2\Delta + \pi\tilde{\Omega}_n} \right], \tag{3.11}$$

$$\beta F = \beta F^{ref} + \beta U^{el} + \frac{\Gamma^3}{3\pi}, \tag{3.12}$$

$$\beta P = \beta P^{ref} - \frac{2\Gamma^3}{3\pi} - \frac{4\beta^*}{\pi} \left(\frac{\pi \tilde{P}_n}{2\Delta + \pi\tilde{\Omega}_n} \right)^2, \tag{3.13}$$

$$\beta \mu_\alpha = \beta \mu_\alpha^{ref} + \beta \Delta \mu_\alpha^{el}, \tag{3.14}$$

where

$$-\Delta\mu_\alpha^{el} = z_\alpha^2 \Gamma_\alpha \left(\Gamma - \frac{\Gamma_\alpha}{2\sigma_\alpha} \delta_{\alpha d} \right) + z_\alpha \Gamma_\alpha \frac{\pi \tilde{P}_n}{2\Delta + \pi\tilde{\Omega}_n} \left(2z_\alpha + \sigma_\alpha \Gamma_\alpha \delta_{\alpha d} \right) - \sigma_\alpha^3 \left(\frac{\pi \tilde{P}_n}{2\Delta + \pi\tilde{\Omega}_n} \right)^2 \left(\Gamma_\alpha \left(1 + \frac{1}{2}\Gamma_\alpha \delta_{\alpha d} \right) - \frac{1}{3} \right), \tag{3.15}$$

where U^{el} is the electrostatic contributions to the internal energy. As usual F and P stand for the Helmoltz free energy and pressure, respectively. The superscript "ref" denotes the corresponding properties of the reference system, which is represented by the same system of particles but with all charges equal to zero. The properties of such reference system were calculated using the thermodynamic perturbation theory of Wertheim [17, 26].

3.3. Monte Carlo Simulation Details

In the present work ordinary canonical Monte Carlo simulations following the standard Metropolis' scheme were used, applying the integrated MC/MD/BD simulation package Molsim [27]. In all cases a total of 40 protein molecules and an equivalent number of counterions and co-ions (the latter determine the concentration of simple electrolyte) to satisfy the electroneutrality condition Eq. 2.2 were placed in the simulation cell. We assume that the configurational energy of the model system is pairwise additive; the pair potentials are given by Eq. 2.2.

To minimize finite system size effects, the Ewald summation method [28] was used. In calculating statistics, averages were collected at least over 200,000 attempted Monte Carlo steps per particle, after an equilibration run of 50,000 configurations.

The various distribution functions were obtained via the histogram method using a 0.02 nm bin width, and a chemical potential of a simple electrolyte by Widom's test particle insertion procedure.

Excess internal energy was calculated very precisely with relative standard deviation less than $1 \cdot 10^{-4}$, and the *first* bin of radial distribution functions was obtained with maximum relative standard deviation less than 0.5%, as well as the excess chemical potential of the simple electrolyte.

4. Results

4.1. Theory Versus Simulations

This section contains comparison between the theoretical results obtained from the integral equation approach based on the PMSA and PHNC approximations and new Monte Carlo simulation data. The calculations are based on the model lysozyme solution (M=17000 g/mol) in presence of 0.1 M sodium chloride. The protein monomer was assumed to be a sphere with diameter $\sigma_p = 34.4$ Å and $Z_p = 14$. The

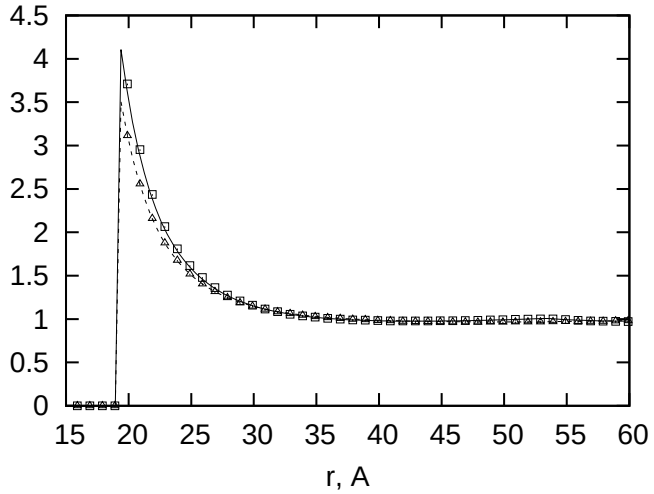

Figure 1. Protein–counterion radial distribution functions of the -14:+1 polyelectrolyte at C_p=100 g/l in mixture with 0.1 M solution of +1:-1 electrolyte. Solid line and squares denote HNC and MC results for fully dimerized case, dashed line and triangles are the polymer HNC and MC results for monomer case.

monovalent counterions and co–ions are spherical particles with diameter 4 Å. It is assumed that the proteins can form dimers; the fraction of dimers in solution was varied from x_p=0, (50%) to 100%. The structure is presented in forms of various distribution functions for protein concentration 100 g/l. Thermodynamic properties (excess internal energy, osmotic pressure, etc) are given as a functions of protein concentration ranging from 10 to 100 g/l. First we present the results for distribution functions given in Figures 1–4.

Center–Center Distribution Functions: In Figure 1 we show the counterion–protein distribution functions as obtained by the Monte Carlo method and the Polymer HNC theory. The squares and full line apply to fully dimerized case x_p=1 and triangles and dotted line to x_p=0 (only monomers present). As expected there is stronger accumulation of counterions around proteins in the case when the latter form dimers. Agreement between the theory and simulation is good.

Next in Figure 2 we present the counterion–counterion distribution function. There is a very small difference in shape for x_p=0 and x_p=1 cases, and for this reason only the results for solution with dimerized

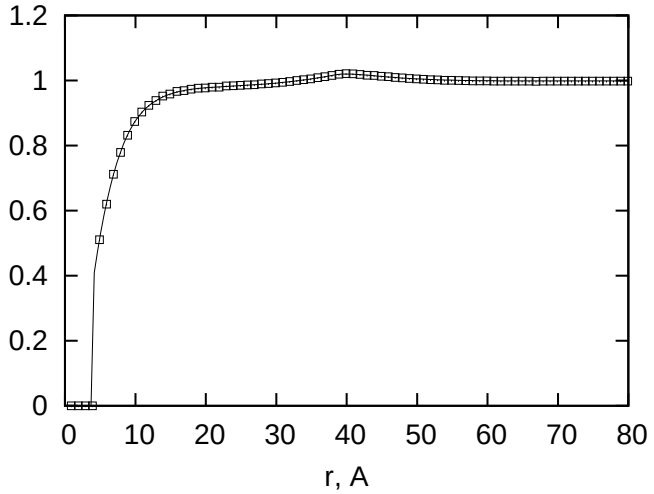

Figure 2. Counterion–counterion radial distribution functions for the same mixture as shown in Fig. 1. Electrolyte concentrations and notation as for Fig. 1.

proteins are shown. A small hump at $r = 40$ Å indicates that counterions are most likely to be distributed on the opposite sides of the protein molecule. Such a shape of the c-c distribution function is typical for highly asymmetric electrolytes and has been noticed before [29, 30].

In contrast to this observation, the co-ion–protein distribution functions displayed in Figure 3 are significantly different in the two (x_p=0 and x_p=1) examples. For fully dimerized case the co-ions are strongly pushed out of the domain of the protein dimer; this is so–called Donnan exclusion effect which causes unequal distribution of electrolyte in the membrane equilibrium experiment (see, for example, [10, 31, 32]).

In Figure 4 we see the resulting protein–protein site–site distribution; only the intermolecular part is shown. We see that dimerized proteins are, as result of twice higher charge, distributed at larger distances from each other than monomers. This result is expected for solutions with monovalent counterions but for more highly coupled systems (low dielectric constant and/or multivalent counterions) the situation may be different as shown before by Hribar and Vlachy [30, 33, 34].

Osmotic Properties: In Figure 5 we show the excess pressure $\Delta P = P - P_{id}$ calculated for a protein–electrolyte mixture as a function of protein concentration (in grams per liter). For this calculation the protein

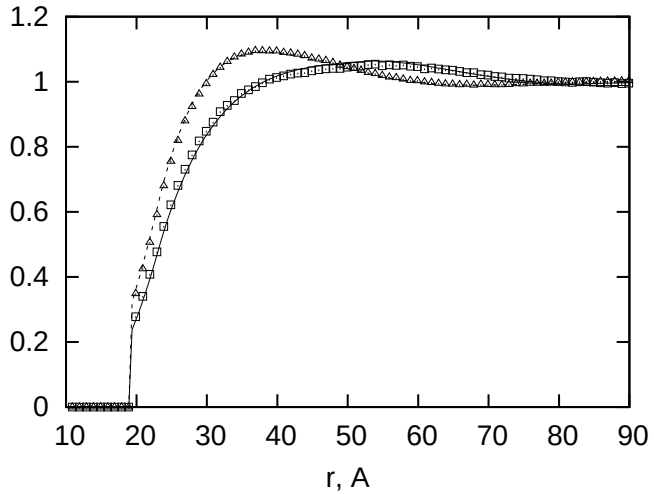

Figure 3. Protein–co-ion distribution functions; the concentrations and notation as for Fig. 1.

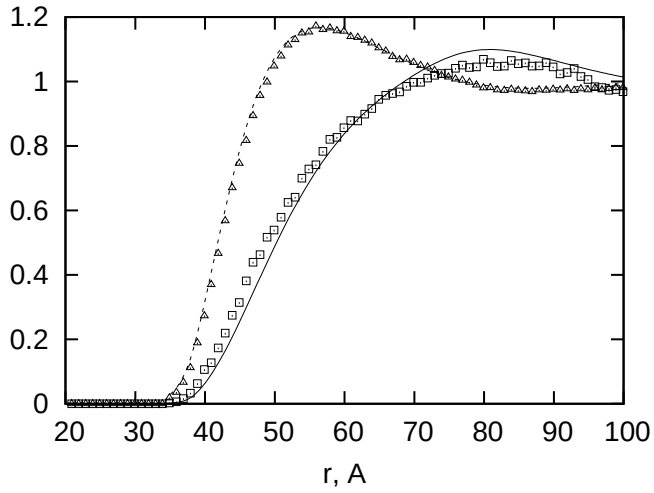

Figure 4. Protein–protein distribution functions. Other as for Fig. 1

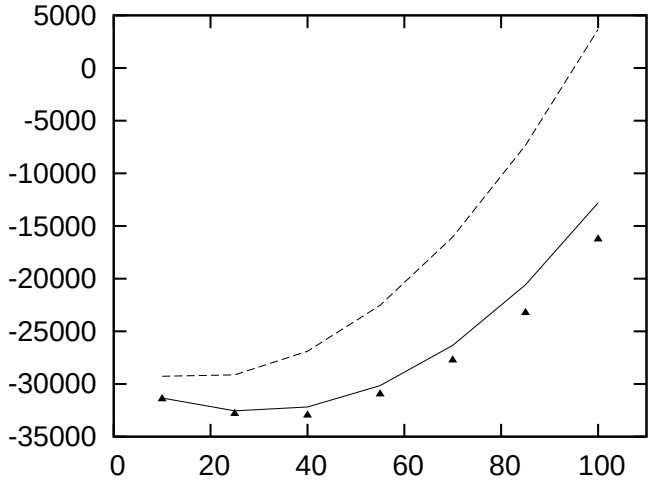

Figure 5. An excess pressure in the mixture of -14:+1 and +1:-1 electrolytes; C_p=100 g/l, while the concentration of simple electrolyte was 0.1 M.

molecules are assumed to be in form of monomers. The polymer HNC and MSA results (the solid and broken lines) together with the Monte Carlo data (symbols) are shown. It is evident from this plot that PMSA approach yield results which are too high with respect to simulations, while the PHNC calculations are quite close to the Monte Carlo results.

Next we present the results for the Donnan pressure. We consider the equilibrium distribution of simple electrolyte between an aqueous protein–electrolyte mixture and an aqueous solution of the same electrolyte. The two solutions are separated by a membrane permeable to water and all small ions but not to the protein molecules. The thermodynamic equilibrium across the membrane requires that for each permeable charged species and water the electrochemical potential is the same on both sides of the membrane. In literature this situation is known as Donnan equilibrium and the resulting Donnan pressure is an important measurable quantity (see, for example, [3,4,6–9]). The experimental Donnan pressure data are often used to identify principal interactions in protein solutions. In theory the Donnan pressure can be evaluated as a difference between the osmotic pressures in the two compartments being in equilibrium as described before. Numerical error associated with such a procedure may be significant since the resulting Donnan pressure is usually much smaller than the two individual osmotic pressures. This is

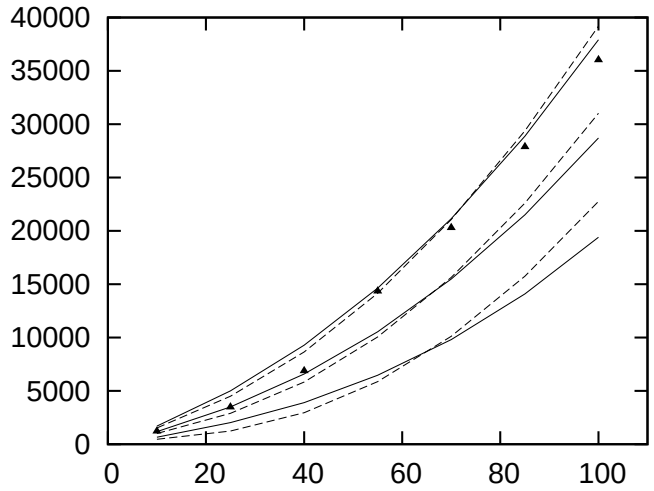

Figure 6. Osmotic pressure for the model lysozyme solutions (with $x_p = 0, 0.5, 1$) as a function of the protein concentration. The concentration of the added +1:-1 electrolyte is 0.1 M. The polymer HNC results are denoted by solid lines, PMSA by dashed lines and MC data by symbols.

especially true when a low-molecular electrolyte is added in excess to the protein.

The results for Donnan pressure are given in Figure 6 as a function of concentration in grams of protein per liter. The concentration of low-molecular +1:-1 electrolyte is 0.1 M in this case. Triangles denote Monte Carlo data for x_p=0, and the full and dotted curves the PHNC and PMSA results for this case. Both theories seem to be in fair agreement with the computer simulation, except perhaps for low protein concentrations. Note that in the latter case the numerical errors are large. In this figure we also present result for cases x_p=0.5, 1 (two lower bands of the curves). The consistency between the two theories is quite encouraging and it also holds for cases with protein dimerization.

Excess Chemical Potential: In Figure 7 the excess chemical potential of simple electrolyte is given as a function of protein concentration and for x_p=0 (top panel – only monomers), x_p=0.5 (center panel), and x_p=1 (bottom panel – only dimers). The PHNC calculation (solid lines) is in better agreement with computer simulations (symbols) for the excess chemical potential; PMSA (broken lines) considerably overestimates this quantity.

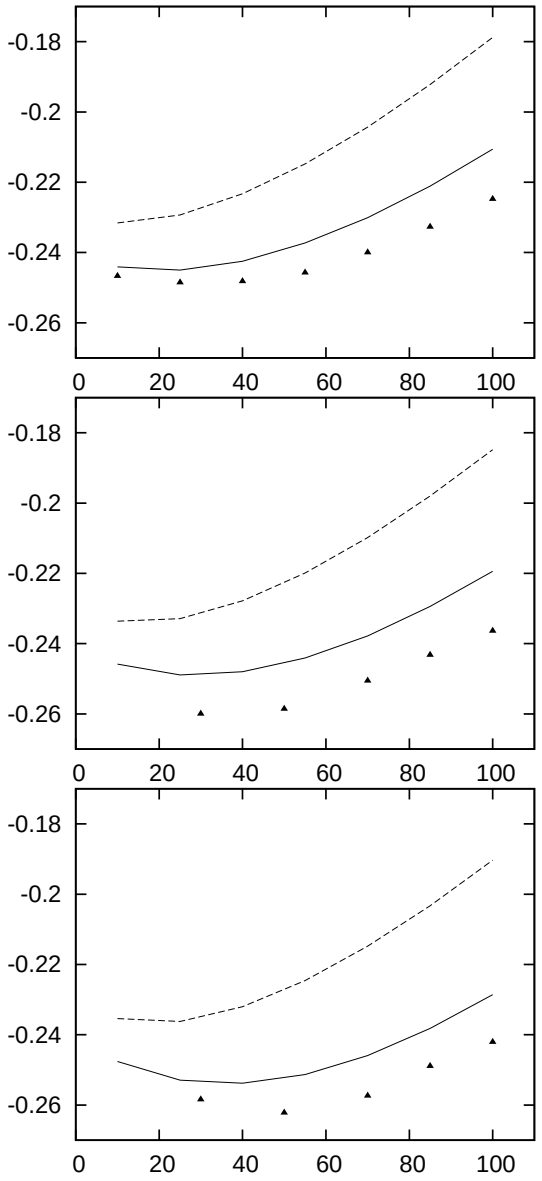

Figure 7. Excess chemical potential of the +1:-1 electrolyte in mixture with the -14:+1 model protein solution. The concentration of +1:-1 electrolyte is 0.1 M. Top panel - 100% monomers (no dimers), center panel - 50% monomers, bottom panel - fully dimerized case.

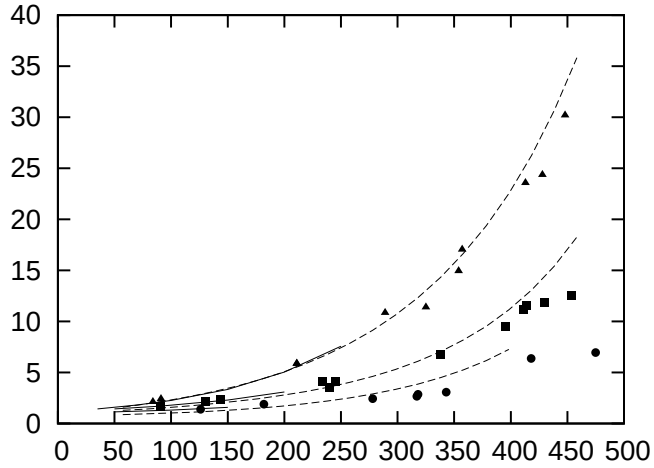

Figure 8. Osmotic coefficients as a function of concentration of BSA in 0.15 M sodium chloride electrolyte. Triangles, squares and circles denote experimental results for pH's 7.3, 5.4 and 4.5 respectively [3]. The solid lines denote the Polymer HNC results and the dashed lines Polymer MSA results.

4.2. Analysis of Experimental Data

This section contains short analysis of experimental results available in literature by using the integral equation theories described in previous chapters.

Bovine Serum Albumin: In Figure 8 we present the results for BSA solutions in mixture with 0.15 M sodium chloride in water at 298 K [3]. These experimental data were analyzed before using different theoretical approaches (see, for example, [4, 35–37]). The results for three different pH values are given; we present the comparison between the experiment (pH=7.3 - triangles, 5.4 - squares, 4.5 - circles), PHNC (solid lines) and PMSA (broken lines). The diameters of counterions and co-ions are assumed to be equal to 4.0 Å in this calculation. The net protein charges Z_p are assumed to be -20.5, -9.3 and 4.1 for pH's 7.3, 5.4 and 4.5 correspondingly.

For pH values 5.4 and 7.3 the analysis indicates small association with fraction of dimers less than 10% (about zero for pH=5.4). The degree of association is larger at pH=4.5 where the best fit is obtained for degree of dimerization equal to 50%.

Human Serum Albumin: Experimental results [8] for aqueous solutions of HSA are fitted to the theoretical ones in Figure 9. Two examples are shown: in top panel we present data for HSA solutions with pH=8.0 (Z_p=-22) and in bottom panel for pH=5.4 (Z_p=0). For simplicity we treat the buffer as +1:-1 size asymmetric electrolyte of the same ionic strength. In order to fit the experimental results the diameters of small ions are chosen to be equal $\sigma_+ = 2.13$ Å and $\sigma_- = 5.5$ Å. Our numerical analysis (best fit) suggests 80% dimerization for pH=8.0 and 100% dimerization for pH=5.4.

Lysozyme Solutions: Similar analysis is for aqueous Lysozyme solutions in two different salts given in Figure 10. In top panel we show the osmotic behavior of Lysozyme in sulphate buffer (ionic strength of buffer is high I=3 M) at pH=4.2 (Z_p=+14) [7]. Again we treat the buffer as +1:-1 size asymmetric electrolyte; the diameters of small ions are $\sigma_+ = 2.13$ Å and $\sigma_- = 4.5$ Å. The fraction of dimers seem to be zero in this case. In center and bottom panel we show the experimental results for phosphate buffer at pH=7 and 8 (Z_p=+8/+7.5) [6], again no dimerization is found. The diameters of ions of simple electrolyte are $\sigma_+ = 2.13$ Å and $\sigma_- = 5.5$ Å.

5. Conclusions

New theoretical and computer simulation results are presented for mixtures of highly asymmetric electrolytes modelling protein solutions. Protein molecules were assumed to exist as monomers and/or as dimers. In monomer forms they are hard spheres with charge in the center. Size and charge of the model protein is chosen to mimic aqueous solutions of Lysozyme. Simple ions which are also present in the system are modelled as charged hard spheres of different sizes but symmetric in charge (+1:-1 electrolyte). In all cases the solvent is modelled as continuous dielectric.

The results for various center–center distribution functions are calculated for mixtures of protein monomers, dimers and +1:-1 simple electrolyte using the Polymer HNC theory. These data are compared with the machine calculations for the same model system. The agreement between theory and Monte Carlo simulations is reasonably good for the range of concentrations and charges studied here.

In addition to structural we also studied thermodynamic parameters of this systems as a function of protein concentration. One of them is the excess free energy for a pair of positive and negative ions. The results indicate that both theories PMSA and PHNC follow qualitatively the trend of computer simulations. They both overestimate value of the excess free energy - polymer HNC is much closer to the Monte Carlo

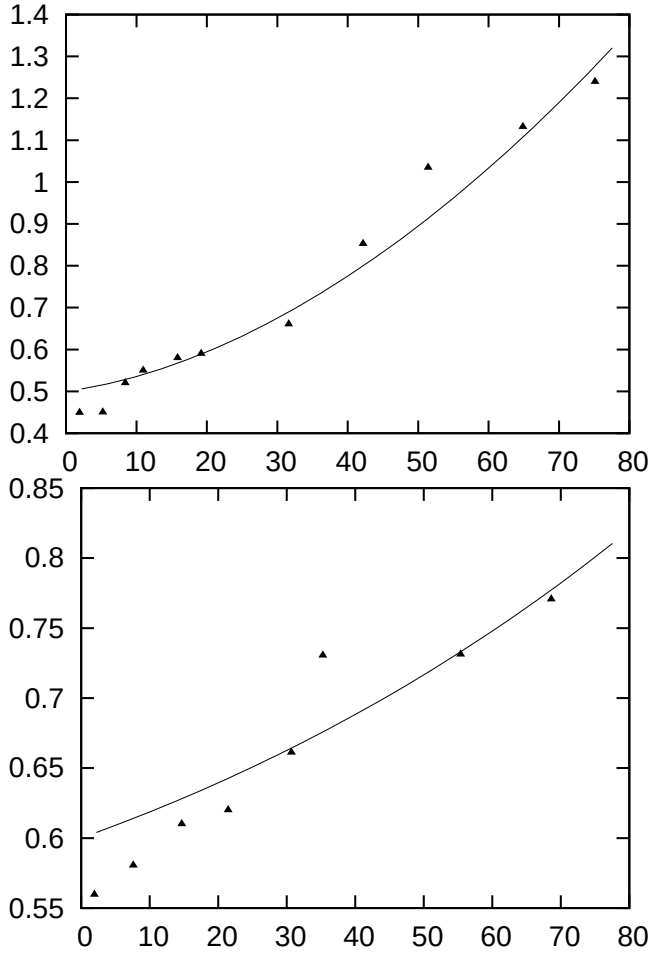

Figure 9. Osmotic coefficient as a function of the HSA concentration in 0.1 M phosphate buffer; pH=8 (top panel), and pH = 5.4 (bottom panel). Lines denote MSA results, symbols are experimental data from [8].

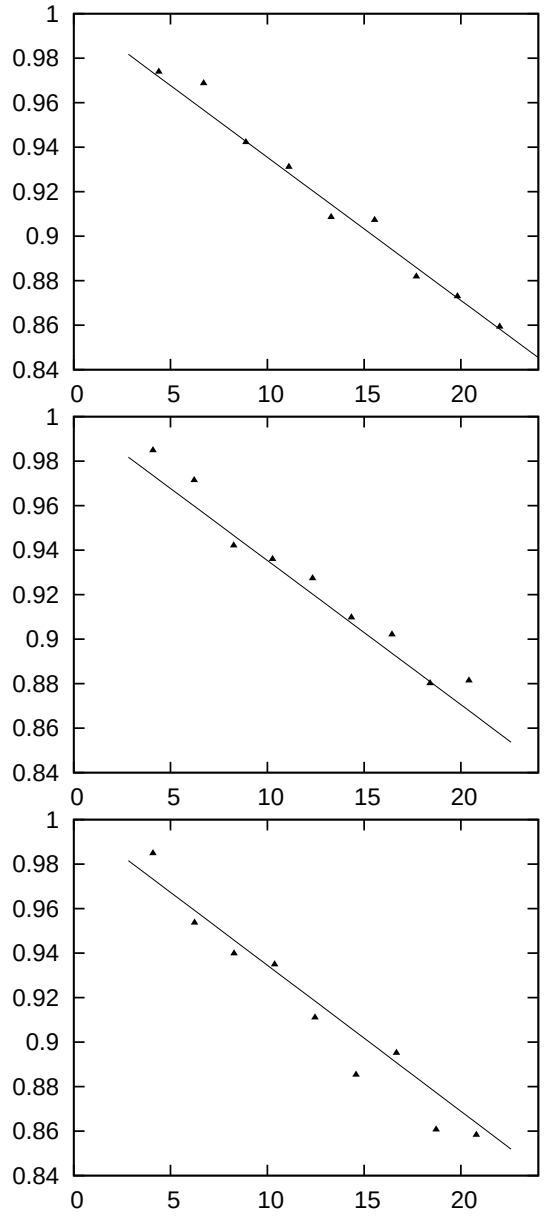

Figure 10. Osmotic coefficient as a function of concentration of lysozyme in 3 M buffer at pH=4.2 (top panel), pH=7.0 (center panel) and 8.0 (bottom panel). Lines denote MSA results, symbols - experimental data from [6, 7].

data than PMSA calculation.

In particular we were interested in the osmotic pressure built across the semi-permeable membrane when on side is protein-electrolyte mixture and just electrolyte on the other. This situation is called Donnan equilibrium and can often been encountered in biology or in technological processes. The theories and simulations are again in fair agreement for this quantity.

The theory was finally applied to analyze the experimental data found in literature. Our analysis indicates that low values of the osmotic pressure found in literature can be rationalized by partial dimerization of the protein molecules. This is of course just one of the possible explanations. The model for the protein–electrolyte mixture used here is namely very crude. The most immediate improvements would require to treat the protein molecules with discrete surface charges and to model more realistically the buffer solutions.

References

1. A.Bhattacharya, P.Ghosh, *Rev. Chem. Engn.* **20**, 111 (2004).
2. G.B.Sukhorukov, A.Fery, M.Brumen, H.Mohwald, *Phys. Chem. Chem. Phys.* **6**, 4078 (2004).
3. V.L.Vilker, C.L.Colton, K.A.Smith, *J.Colloid. Interface Sci.* **79**, 548 (1981).
4. C.A.Haynes, K.Tamura, H.R.Korfer, H.W.Blanch, J.M.Prausnitz, *J. Phys. Chem.* **96**, 95 (1992).
5. A.George, W.W.Wilson, *Acta Cristallog.* **D50**, 361 (1994).
6. Y.U.Moon, R.A.Curtis, C.O.Anderson, H.W.Blanch, J.M.Prausnitz, *J. Solution Chem.* **29**, 699 (2000).
7. Y.U.Moon, C.O.Anderson, H.W.Blanch, J.M.Prausnitz, *Fluid Phase Eq.* **168**, 229 (2000).
8. J.Rescic, V.Vlachy, A.Jamnik, O.Glatter, *J. Colloid Interface Sci.* **239**, 49 (2001)
9. Y.Z.Lin, Y.G.Li, Y.F.Lu, *Acta Chim. Sinica* **59**, 2110 (2001).
10. G.Kortüm 1965. *Treatise on Electrochemistry* pp. 389-94. London/New York: Elsevier.
11. R.Piazza, *Curr. Opin. Coll. Interface Sci.* **8**, 512 (2004).
12. R.A.Curtis, J.Ulrich, A.Montaser, J.M.Prausnitz, H.W.Blanch, *Biotechnology & Bioenginnering* **79**, 367 (2002).
13. F.W.Tavares, D.Bratko, J.M.Prausnitz, *Current Opinion Coll. Interface Sci.* **9**, 81 (2004).
14. C.Haas, J.Drenth, W.W.Wilson *J. Phys. Chem. B.* **103**, 2808 (1999).

15. Yu.V.Kalyuzhnyi, V.Vlachy *J. Chem. Phys.* **108**, 7870 (1998).
16. P.J.Rossky, R.A.Chiles, *Mol. Phys.* **51**, 661 (1984).
17. M.S.Wertheim, *J. Stat. Phys.* **35**, 19 (1984).
18. Yu.V.Kalyuzhnyi, P.T.Cummings, *J. Chem. Phys.* **104**, 3325 (1996).
19. P.Attard *Mol. Phys.* **83**, 273 (1994).
20. M.F.Holovko, Yu.V.Kalyuzhnyi, *Mol. Phys.* **73**, 1145 (1991).
21. Yu.V.Kalyuzhnyi, P.T.Cummings, *J. Chem. Phys.* **115**, 540 (2001); *ibid.* **116**, 8637 (2002).
22. L.Blum, *Mol. Phys.* **30**, 1529 (1975).
23. L.Blum, J.Høye, *J. Phys. Chem.* **81**, 1311 (1977).
24. O.Bernard, L.Blum, *J. Chem. Phys.* **104**, 4746 (1996).
25. O.Bernard, L.Blum, *J. Chem. Phys.* **112**, 7227 (2000).
26. M.S.Wertheim, *J. Chem. Phys.* **85**, 2929 (1986).
27. P. Linse, *Molsim 3.6.7.*, Lund University, Sweden (2004).
28. M.P.Allen, D.J.Tildesley, 1989. *Computer Simulations of Liquids*, Oxford University Press, New York.
29. V.Vlachy, C.H.Marshall, A.D.J.Haymet *J. Am. Chem. Soc.* **111**, 4160 (1989).
30. V.Vlachy, *Annu. Rev. Phys. Chem.*,**502**, 145 (1999).
31. B.Hribar, V.Vlachy, L.B.Bhuiyan, C.W.Outhwaite *J. Phys. Chem. B.* **104**, 11522 (2000).
32. V.Vlachy, *Langmuir* **17**, 399 (2001).
33. B.Hribar, V.Vlachy, *J. Phys. Chem. B* **101**, 3457 (1997).
34. B.Hribar, V.Vlachy, *Biophys. J.* **78**, 694 (2000).
35. V.Vlachy, J.M.Prausnitz, *J. Phys. Chem.* **96**, 6465 (1992).
36. Yu.V.Kalyuzhnyi, J.Rescic, V.Vlachy, *Acta Chim. Slov.* **45**, 199 (1998).
37. V.Vlachy, B.Hribar, J.Rescic, Yu.V.Kalyuzhnyi, in *Ionic Soft Matter: Modern Trends in Theory and Applications*, NATO Science Series II: Mathematics, Physics and Chemistry; D.Henderson, M.Holovko, A.Trokhymchuk, (Eds.), Springer, vol. 206, July 2005.

Препринти Інституту фізики конденсованих систем НАН України розповсюджуються серед наукових та інформаційних установ. Вони також доступні по електронній комп'ютерній мережі на WWW-сервері інституту за адресою http://www.icmp.lviv.ua/

The preprints of the Institute for Condensed Matter Physics of the National Academy of Sciences of Ukraine are distributed to scientific and informational institutions. They also are available by computer network from Institute's WWW server (http://www.icmp.lviv.ua/)

Максим Юрійович Дручок
Юрій Володимирович Калюжний
Юрій Рещіч
Войко Влахі

Аналіз даних для осмотичного тиску водних розчинів протеїнів на основі багатокомпонентної моделі

Роботу отримано 25 жовтня 2005 р.

Затверджено до друку Вченою радою ІФКС НАН України

Рекомендовано до друку семінаром відділу теорії розчинів

Виготовлено при ІФКС НАН України